AIAA JOURNAL
Vol. 30, No. 2, February 1992

Finite Element Analysis of Oscillatory Flow with Heat Transfer Inside a Square Cavity

B. Ramaswamy,* T. C. Jue,† and J. E. Akin‡
Rice University, Houston, Texas 77251

In this work, a semi-implicit projection-type finite element method is applied to solve the incompressible oscillatory cavity flow with heat transfer. The two-dimensional, time-dependent Navier-Stokes and energy equations are numerically integrated by a time-split Galerkin finite element method using direct matrix solvers. The time accuracy of the method was tested by calculating the transient buoyancy-driven flow in a square cavity with differentially heated vertical walls. The oscillatory cavity flow is then studied considering the effects of heat transfer, Reynolds number, and oscillatory Stokes number to measure the stability of the scheme for such a high singularity phenomenon. The proposed scheme is found to be stable and convergent for high Rayleigh numbers, and will be applicable to general problems involving flow and heat transfer, especially in three dimensions.

Nomenclature

$g1$ = prescribed velocity vector
$g2$ = prescribed temperature
h = height of the cavity
p = dimensionless pressure
p^* = dimensional pressure
q = weighting function
Pr = Prandtl number
Ra = Rayleigh number
Re = Reynolds number
t = dimensionless time
t^* = dimensional time
Δt = time increment
U = characteristic velocity
u,v = velocity components in x and y directions
v = weighting function
(x,y) = Cartesian coordinate
α = thermal diffusivity
β = oscillatory Stokes number
$\tilde{\beta}$ = thermal expansion coefficient
Γ = piecewise smooth boundary of the domain Ω
θ = dimensionless temperature
θ^* = dimensional temperature
$\tilde{\theta}^*$ = weighting function
μ = viscosity coefficient
ν = kinematic viscosity coefficient
Ω = bounded domain in R^2
ω = frequency of the oscillation

Superscripts

n = quantities at time t^n
T = transpose
$\tilde{}$ = auxiliary value
$\hat{}$ = auxiliary value

Subscript

0 = initial value

Received Nov. 27, 1990; presented as Paper 91-0122 at the AIAA 29th Aerospace Sciences Meeting, Reno, NV, Jan. 7-10, 1991; revision received June 17, 1991.

*Assistant Professor, Department of Mechanical Engineering and Materials Science.
†Graduate Student, Department of Mechanical Engineering and Materials Science.
‡Professor, Department of Mechanical Engineering and Materials Science.

I. Introduction

THE solution of practical fluid flow problems by finite element method has received increasing attention during recent years. In particular, the solution of incompressible fluid flow phenomena with and without heat transfer can now be performed efficiently in many practical cases. Such potential originates in its ease in handling very complex geometries and the ability to incorporate differential-type boundary conditions naturally. Among available combinations of the solution variables, the method using primitive variables is considered important primarily because these variables are more physical and have lower order equations, and this form of equation provides a relatively straightforward extension to three dimensions. However, the primitive-variable formulation has difficulties with the determination of pressure, which has no time term, and is coupled implicitly with the divergence-free constraint on the velocity. This constraint, which is the continuity constraint equation, prohibits time integration of the incompressible flow equations in a straightforward manner. This is one of the major differences from compressible flow calculations.

The most primitive formulation for the incompressible Navier-Stokes equations is constructed by the mixed formulation[1] where the velocity components and the pressure are used as variables. The coupled equation system of the incompressibility equation and the Navier-Stokes equations can be solved simultaneously[2] by such a direct solver as the LU decomposition or the Gauss elimination. The use of same interpolation for the velocity and for the pressure generates parasitic pressure. These elements do not satisfy the *inf-sup* condition of Babuska-Brezzi, as discussed in Ref. 3. Therefore, various mixed finite element approximations have been developed recently. Usually, the order of the interpolation function for the velocity is chosen higher than that of the pressure to obtain physically reasonable solutions. For example, the multilinear interpolation function for the velocity and the piecewise-constant one for the pressure are commonly used in the mixed formulation. However, this element occasionally yields spatial oscillation under particular boundary conditions.

The penalty method[4-7] is a variation of the mixed formulation. In this method it is assumed that the pressure equals the negative of a penalty parameter times the continuity equation. This expression is then substituted into the pressure gradient terms in the Navier-Stokes equation and pressure is eliminated. The resulting equations are solved for the velocity components using the finite element method. The penalty parameter must be made large enough to enforce continuity,

but not so large that the other terms in the Navier-Stokes equations are calculated inaccurately. The pressure is then recovered from the initial relation. In this approach, the velocity and pressure should also be approximated by the interpolation functions which are consistent with the Babuska-Brezzi condition. This problem can be resolved using a lower order integration for the terms associated with the penalty function.[8] It should be noted that the reduced integration technique for the penalty term leads to inconsistent imposition of incompressibility constraint, since the incompressibility cannot be retained in the discretized system as explained by Engelman et al.[9]

On the other hand, low- and same-order elements are very attractive for their programming simplicity, and the purpose of this paper is to develop a stable and efficient method using bilinear quadrilateral elements. The present effort is restricted to present a modification to the existing velocity correction algorithms[10-14] that reduces the restrictions on the time step with simultaneous reduction in computing effort at each time step. In the following sections of this paper more details about the theory and numerical methods used in the program for laminar flow with heat transfer are given. We consider two numerical tests: transient buoyancy-driven flow in a square cavity with differentially heated vertical walls, and oscillatory flow with heat transfer. Although the present results are restricted to square cavities of limited aspect ratio, Prandtl number, Reynolds number, and Rayleigh number, the procedure is general and can be equally applied to various complex problems.[15,16] In particular, this method will be cost effective for three-dimensional problems, which are getting more and more important in recent days.

II. Problem Formulation

In this study, the fluid is considered to be viscous and incompressible, and the flow is laminar. The geometry enclosing the flow domain is considered to be a two-dimensional square cavity. The equations to be solved are derived from the basic physical conservation principles of mass, momentum, and energy. Let Ω be a bounded domain in R^2 and T be a positive real number. The spatial and temporal coordinates are denoted by $(x,y) \in \bar{\Omega}$ and $t \in [0, T]$ where a superposed bar indicates the set closure. These generic equations can be written for the velocity [$\boldsymbol{u} = (u, v)^T$], kinematic pressure ($p$, pressure divided by density), and temperature θ in the bounded domain Ω:

$$a\frac{\partial u}{\partial t} + b\left(u\frac{\partial u}{\partial x} + v\frac{\partial u}{\partial y}\right) = -\frac{\partial p}{\partial x} + c\left(\frac{\partial^2 u}{\partial x^2} + \frac{\partial^2 u}{\partial y^2}\right) \text{ in } \Omega \tag{1}$$

$$a\frac{\partial v}{\partial t} + b\left(u\frac{\partial v}{\partial x} + v\frac{\partial v}{\partial y}\right) = -\frac{\partial p}{\partial y} + c\left(\frac{\partial^2 v}{\partial x^2} + \frac{\partial^2 v}{\partial y^2}\right) + s\theta \text{ in } \Omega \tag{2}$$

$$f\frac{\partial \theta}{\partial t} + d\left(u\frac{\partial \theta}{\partial x} + v\frac{\partial \theta}{\partial y}\right) = e\left(\frac{\partial^2 \theta}{\partial x^2} + \frac{\partial^2 \theta}{\partial y^2}\right) \text{ in } \Omega \tag{3}$$

$$\frac{\partial u}{\partial x} + \frac{\partial v}{\partial y} = 0 \text{ in } \Omega \tag{4}$$

where coefficients a, b, c, d, e, and f are assumed different values for problems considered in this work and are listed in Table 1.

The governing equations, Eqs. (1-4) are elliptic in spatial coordinates and parabolic in space and time. Therefore, in order to formulate a well-posed problem, the boundary conditions must be specified for all boundaries and an initial condition for the velocities in the domain of investigation is needed. Let Γ be a piecewise smooth boundary of the domain Ω. The following boundary conditions are specified for the subsets of Γ for two different problems considered in this work:

Table 1 Coefficients of the governing equations

	a	b	c	d	e	f	s
Thermally driven cavity	1	1	Pr	1	1	1	$RaPr$
Oscillating cavity	β	Re	1	Re	$1/Pr$	β	$Ra/(PrRe)$

1. *The thermally driven cavity*

$$u = v = 0, \quad \theta = 0.5, \quad (x = 0)$$

$$u = v = 0, \quad \theta = -0.5, \quad (x = 1)$$

$$u = v = 0, \quad \frac{\partial \theta}{\partial y} = 0, \quad (y = 0)$$

$$u = v = 0, \quad \frac{\partial \theta}{\partial y} = 0, \quad (y = 1)$$

2. *Oscillatory cavity flow with heat transfer*

$$u = v = 0, \quad \theta = -0.5, \quad (x = 0)$$

$$u = v = 0, \quad \theta = -0.5, \quad (x = 1)$$

$$u = v = 0, \quad \theta = -0.5, \quad (y = 0)$$

$$u = cost, \quad v = 0, \quad \theta = 0.5, \quad (y = 1)$$

III. Spatial Discretization

A weak formulation of Eqs. (1-4) is obtained by multiplying the differential equation with a suitable weighting function and integrating over Ω. Let $H^1(\Omega)^d$ denote the standard Sobolev space of vector functions defined on $\Omega \subset R^d$ which are square integrable and have square-integrable first-order derivatives with respect to the spatial coordinates. Furthermore, let $L^2(\Omega)$ be the Hilbert space of scalar square-integrable functions. We multiply the momentum equations by the weighting function $\boldsymbol{v} \in H^1(\Omega)^d$, $\boldsymbol{v}|_{\Gamma_g} = 0$, the energy equation by the weighting function $\tilde{\theta} \in H^1(\Omega)^d$, and the continuity equation by the weighting function $q \in L^2(\Omega)$, see e.g., Ref. 17, and then integrate over Ω. After integration by parts of the stress term, applying the divergence theorem and the boundary conditions, the following weak form of the original problem is obtained: Given the proper boundary and initial conditions, find $\boldsymbol{u}(\boldsymbol{x},t) \in H^1(\Omega)^d$, $\theta \in H^1(\Omega)^d$, and $p(\boldsymbol{x},t) \in L^2(\Omega)$ such that

$$\left(a\frac{\partial \boldsymbol{u}}{\partial t}, \boldsymbol{v}\right) + (b(\boldsymbol{u}\cdot\nabla)\boldsymbol{u}, \boldsymbol{v}) = (\nabla p, \boldsymbol{v}) - c(\nabla^2 \boldsymbol{u}, \boldsymbol{v}) + (s, \boldsymbol{v}), \forall \boldsymbol{v} \in H^1(\Omega)^d, \boldsymbol{v}|_{\Gamma_{g1}} = 0 \tag{5}$$

$$\left(f\frac{\partial \theta}{\partial t}, \tilde{\theta}\right) + (d(\boldsymbol{u}\cdot\nabla)\theta, \tilde{\theta}) = e(\nabla^2 \theta, \tilde{\theta}), \forall \tilde{\theta} \in H^1(\Omega)^d, \tilde{\theta}|_{\Gamma_{g2}} = 0 \tag{6}$$

$$(\nabla \cdot \boldsymbol{u}, q) = 0, \forall q \in L^2(\Omega) \tag{7}$$

$$\boldsymbol{u}|_{\Gamma_{g1}} = \boldsymbol{g1} \tag{8}$$

$$\theta|_{\Gamma_{g2}} = \boldsymbol{g2} \tag{9}$$

$$\boldsymbol{u}(\boldsymbol{x},0) = \boldsymbol{u}_0(\boldsymbol{x}) \tag{10}$$

The fully discrete form of Eqs. (5–10) are obtained by discretizing the domain Ω into nonoverlapping subregions called finite elements. In each element the unknown fields are approximated by simple polynomial functions. We note that $\boldsymbol{u}$ and $\theta \in H^1(\Omega)^d$ implies that the interpolation of the velocity and temperature must be continuous across interelement boundaries, whereas $p \in L^2(\Omega)$ means that the pressure interpolation can be discontinuous.

When the finite element approximation is applied to Eqs. (5–10) by the Galerkin method, it yields nonlinear simultaneous ordinary differential equations of the form

$$aM\frac{dU}{dt} + HP + cS(U) + bK(U)U = F_1 \qquad (11)$$

$$fM\frac{d\Theta}{dt} + dK(U)\Theta + eS(\Theta) = F_2 \qquad (12)$$

and

$$DU = 0 \qquad (13)$$

where M,$K(U)$,S,H, and $D = H^T$ are mass, convection, diffusion, pressure gradient, and divergence matrices, respectively. Vectors U, Θ, and P represent finite element solutions for velocity, temperature, and pressure, respectively. The right-hand side vectors F_1 and F_2 result from the imposition of natural boundary conditions and the exertion of a body force.

IV. Temporal Discretization

Many scientists think that the finite element method has at least a theoretical edge over the finite difference method. Nevertheless, finite difference solutions of time-dependent hydrodynamic problems have been applied much more successfully in computational fluid dynamics than in finite element solutions. One reason is that finite difference solutions of the initial value problem are most cost effective. Another reason is that the Navier-Stokes equations have been solved by the finite difference method since the early 1960s, whereas finite element method solutions have appeared since the late 1970s. This fact leads to the assumption that finite difference codes in computational fluid dynamics are more developed than finite element codes. Although many sophisticated and large-scale analysis methods have been proposed with the progress of computers, the transient three-dimensional analysis of flow remains to be a difficult task both in finite difference and finite element methods because of the enormous amount of computational storage requirement and CPU cost. In order to overcome these difficulties, various kinds of computational strategies have been proposed, especially regarding time integration schemes.[18–20] The time integration schemes can be classified into the explicit method and implicit method. The former has an advantage in computational storage, while the time step must be small enough to satisfy the stability condition. On the other hand, the latter is not restricted by the stability condition usually, but the inversions and storage of large matrices are required in the process of the time integration. Therefore, the most eligible time integration should be adopted for each problem, taking the characteristic feature of the problem into account. The transient flow of incompressible viscous fluid is characterized by the hyperbolic, parabolic, and elliptic properties. The hyperbolic and parabolic properties result from the convective and diffusive terms of the Navier-Stokes equations, respectively, and the elliptic property is due to the incompressibility of fluid. Therefore, it is very natural to decompose the time integration of the incompressible Navier-Stokes equations into three separated steps. Such decomposition was originally proposed by Chorin[21] in the finite difference context and was named as the "fractional step" method on which the present time integration scheme is based principally. That is, the incompressible Navier-Stokes equations are decomposed into the hyperbolic, parabolic, and elliptic equations, and each equation is integrated fractionally by different suitable time integration schemes. In the present scheme, the hyperbolic convective equation is temporally integrated using a two-step Adams-Bashforth scheme to save the computational efforts. The fully implicit time integration is used for the incompressibility equation, because the fluid is always incompressible. The same time integration scheme is applied to the time integration of the pressure gradient term, since the pressure plays the role of the Lagrange multiplier for the incompressibility constraint from the viewpoint of the variational principle. Such time integration yields the elliptic pressure Poisson equation, which is solved by the direct solvers. The diffusion equations are integrated temporally via the implicit backward Euler scheme. The underlying philosophy of the present study is to reduce the computational costs as much as possible, daring to sacrifice the accuracy. The authors believe the fractional step method is the most suitable for this purpose, not only because the algorithm can be constructed on a semi-implicit and iterative base, which naturally requires less storage resources than a fully implicit and direct base, but also because the CPU time would be reduced by utilization of an appropriate time integration scheme for each equation. The resulting algorithm is the following:

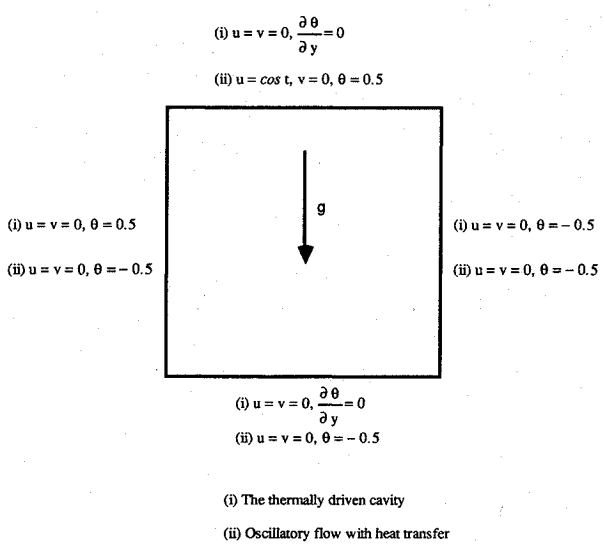

Fig. 1 Problem definition for (i) natural convection and (ii) oscillatory cavity flow with heat transfer.

Step 1: Advection Phase

In this phase, only the convective terms in the momentum equation [Eqs. (1) and (2)] are considered in vector form:

$$a\frac{\partial \boldsymbol{u}}{\partial t} + b(\boldsymbol{u}\cdot\nabla)\boldsymbol{u} = s\theta \qquad (14)$$

This phase allows us to determine an intermediate velocity field $\hat{U}^{n+1}$ from U^n starting with U_0 for $n = 0$, using the explicit Adams-Bashforth method for the nonlinear convective terms

$$aM_D\hat{U}^{n+1} = aMU^n - b\Delta t[\tfrac{3}{2}K(U^n)U^n - \tfrac{1}{2}K(U^{n-1})U^{n-1}] + \Delta tsM\Theta^n \qquad (15)$$

where M_D is the diagonalized mass matrix obtained simply by summing across each row of the consistent mass matrix M and placing the results in the diagonal.

Step 2: Viscosity Phase

This phase considers the viscosity term of the Navier-Stokes equations:

$$a\frac{\partial \boldsymbol{u}}{\partial t} = c\nabla^2 \boldsymbol{u} \tag{16}$$

A first-order implicit Euler time integration scheme is used here and a new intermediate velocity $\tilde{U}^{n+1}$ is determined from $\hat{U}^{n+1}$ by

$$aM\tilde{U}^{n+1} = aM\hat{U}^{n+1} - c\Delta t S(\tilde{U}^{n+1}) \tag{17}$$

In this phase, the boundary conditions of prescribed velocity [Eq. (8)] are applied along the whole boundary

$$\tilde{U}^{n+1}|_{\Gamma_{g1}} = \boldsymbol{g}^{n+1} \tag{18}$$

In cases where a Neumann condition occurs, a surface term is present in Eq. (17).

Step 3: Pressure Phase and Incompressibility

In this phase, the final velocity field U^{n+1} is determined from the intermediate velocity $\tilde{U}^{n+1}$ by adding the dynamic effect of the pressure P^{n+1} determined so that the incompressibility condition remains satisfied. From Eqs. (1) and (2), the pressure phase reads

$$a\frac{\partial \boldsymbol{u}}{\partial t} = \nabla p \tag{19}$$

and is associated with the continuity Eq. (4). Using a first-order implicit Euler scheme in time, one has

$$a\frac{M(\boldsymbol{U}^{n+1} - \tilde{U}^{n+1})}{\Delta t} + HP^{n+1} = 0 \tag{20}$$

and

$$D\boldsymbol{U}^{n+1} = 0 \tag{21}$$

The above represents a system of coupled equations for the final velocity and pressure. It can be written as a symmetric system of linear equations for the scalar P^{n+1}, which can be solved by the same direct elimination method satisfying continuity to machine accuracy:

$$DM_D^{-1}HP^{n+1} = -aD\tilde{U}^{n+1}/\Delta t \tag{22}$$

Boundary conditions for Eq. (22) are imposed values where the pressure is known. Where velocities are imposed Eq. (20) gives

$$\frac{\partial P}{\partial n} = \boldsymbol{n}\cdot\frac{a}{\Delta t}(\tilde{U}^{n+1} - \boldsymbol{U}^{n+1}) = 0 \tag{23}$$

provided that the same boundary values are used for $\tilde{U}$ and $\boldsymbol{U}$ fields. Once the pressure has been obtained, then the final velocity is computed:

$$\boldsymbol{U}^{n+1} = \tilde{U}^{n+1} - a(\Delta t M_D^{-1}HP^{n+1} + F_1^{n+1}) \tag{24}$$

Step 4: Temperature Phase

At first we consider the convection terms in the energy equation:

$$f\frac{\partial \theta}{\partial t} + \mathrm{d}(\boldsymbol{u}\cdot\nabla)\theta = 0 \tag{25}$$

Using Adams-Bashforth method the following equation for convection step can be obtained:

$$fM_D\tilde{\Theta}^{n+1} = fM_D\Theta^n - \mathrm{d}\Delta t[\tfrac{3}{2}K(\boldsymbol{U}^n)\Theta^n - \tfrac{1}{2}K(\boldsymbol{U}^{n-1})\Theta^{n-1}] \tag{26}$$

The final temperature can be obtained by considering a first-order implicit Euler time integration scheme for the conduction terms.

$$fM_D\Theta^{n+1} = fM_D\tilde{\Theta}^{n+1} + e\Delta t S\Theta^{n+1} + F_2^{n+1} \tag{27}$$

The boundary conditions of prescribed temperature are applied along the whole boundary.

V. Numerical Examples

A. Thermally Driven Cavity

Buoyancy-driven flows in an enclosure have received considerable interest in recent years either for practical or numerical analysis reasons. Although most of the problems are fully three-dimensional and time dependent, the limitations imposed by both experimental and theoretical techniques have forced researchers to analyze only those fluid motions that are believed to lend themselves to approximation by two-dimensional models, see e.g., Refs. 22 and 23. The Navier-Stokes and energy equations describing these phenomena are highly nonlinear, and the strong coupling between the equations makes it difficult to obtain analytical solutions as well as becomes a challenging numerical test problem.

The problem of interest here is the unit square cavity containing a viscous fluid. The nondimensional governing equations represent two-dimensional, unsteady, laminar natural convection, where the Boussinesq approximation that density variation is negligible except in the body force term $s\theta$, where temperature-induced variations give rise to a buoyancy term that contributes to fluid motion, is used. The nondimensional transformation used here includes defining a reference velocity

$$U = \frac{\alpha}{h}$$

and the following dimensionless variables

$$u_i = u_i^*/U$$

$$\theta = (\theta^* - \theta_r^*)/(\theta_h^* - \theta_c^*)$$

where θ_r^* is the reference temperature

$$x_i = x_i^*/h$$

$$p = p^*h^2/(\mu\alpha)$$

$$t = t^*\alpha/h^2$$

The dimensionless parameters are defined as the Rayleigh number

$$Ra = \frac{\rho\tilde{\beta}g(\theta_h^* - \theta_c^*)h^3}{\mu\alpha}$$

and the Prandtl number

$$Pr = \frac{\nu}{\alpha}$$

Using the above nondimensionalized parameters, Eqs. (1–4) with the proper boundary conditions are solved by the algorithm listed in Sec. III and IV. The problem definition is

shown in Fig. 1i. Generally stable and accurate numerical solutions are difficult to obtain for laminar flow with $Ra > 10^6$. In this calculation Prandtl number is kept constant at 1.0 and the Rayleigh number is assumed the following range of values: 10^3, 10^4, 10^5, 10^6, 10^7. Computed results are shown in Figs. 2 and 3.

In Table 2, results obtained from present method are compared with those of De Vahl Davis[24] and indicate that the computed solutions are good in agreement over a wide range of Rayleigh numbers. Table 3 compares the maximum values of the vertical velocities obtained from the present work with three benchmark-type results reported in the literature[24-27] where care has been taken to ensure good accuracy of the numerical results.

B. Oscillatory Flow with Heat Transfer

In the oscillatory square cavity with heat transfer, the upper wall oscillates with a maximum amplitude U, which is used as the characteristic velocity. The nondimensional transformation is made by using the following dimensionless variables

$$u_i = u_i^*/U$$

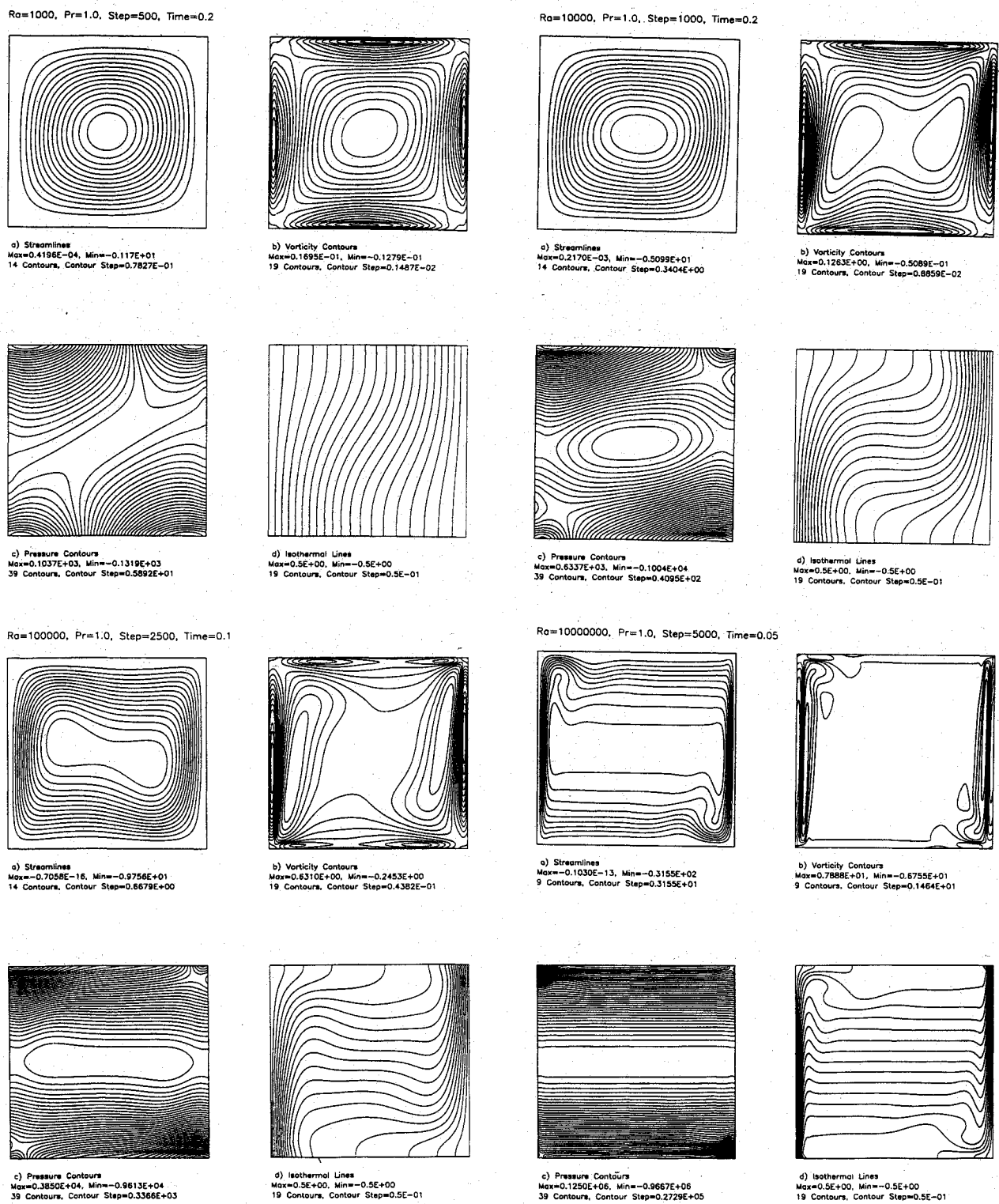

Fig. 2 Steady-state solutions for natural convection flow in a square cavity.

$$x_i = x_i^*/h$$
$$p = p^*h/U\rho\nu$$
$$t = t^*\omega$$
$$\beta = \omega h^2/\nu$$

and the temperature is nondimensionalized as before. All of the results reported in this subsection were started with zero velocity and temperature-initial fields.

In this problem, the flow is characterized by four parameters; Re, β, Ra, and Pr. In this study, the problem is divided

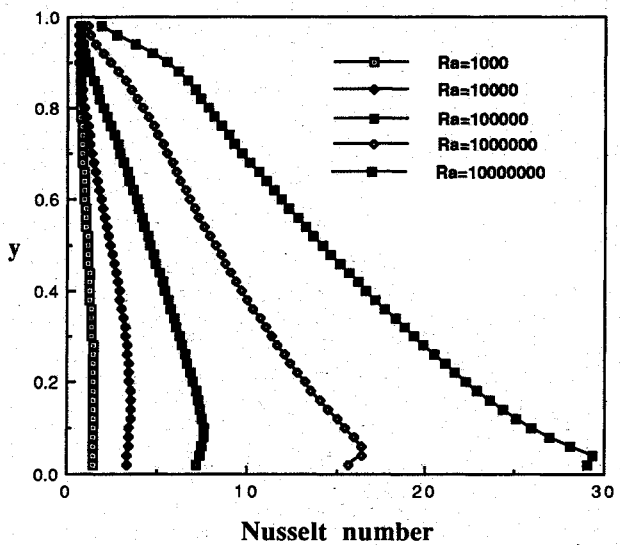

Fig. 3 Hot wall Nusselt number for the square cavity.

Table 2 Cavity center and maximum stream function magnitudes for heated cavity

	Present method		De Vahl Davis (81 × 81 uniform grid)	
Ra	$\lvert\Psi_{mid}\rvert$	$\lvert\Psi_{max}\rvert$	$\lvert\Psi_{mid}\rvert$	$\lvert\Psi_{max}\rvert$
10^3	1.170	1.170	1.170	1.170
10^4	5.099	5.099	5.071	5.071
10^5	9.217	9.756	9.111	9.612
10^6	16.682	17.420	16.320	16.750
10^7	29.436	31.550	No data	No data

Table 3 Comparison of calculated maximum vertical velocity for natural convection in a square cavity

Ra	Source	Maximum vertical velocity
10^4	De Vahl Davis[24]	19.62
	Markatos and Pericleous[27]	19.44
	Le Quere and De Roquefort[26]	19.63
	Present method	19.62
10^5	De Vahl Davis	68.59
	Markatos and Pericleous	69.08
	Le Quere and De Roquefort	68.65
	Present method	68.62
10^6	De Vahl Davis	219.36
	Markatos and Pericleous	221.80
	Le Quere and De Roquefort	220.57
	Present method	232.97
10^7	De Vahl Davis	No data
	Markatos and Pericleous	No data
	Le Quere and De Roquefort	699.30
	Present method	717.04

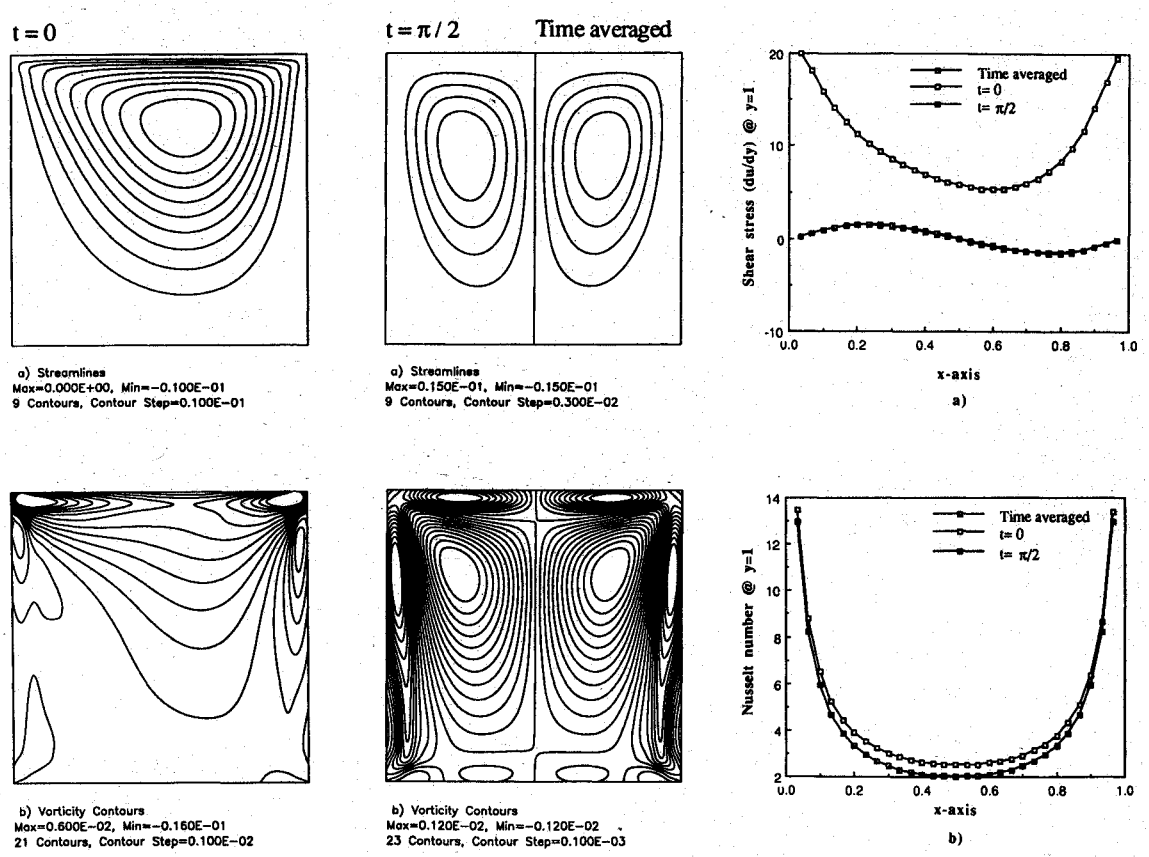

Fig. 4 Oscillatory cavity flow with heat transfer at $t = 0$, $\pi/2$, time-averaged, moving wall shear-stress distribution, and Nusselt number for $Ra = 10^2$, $Pr = Re = \beta = 1$.

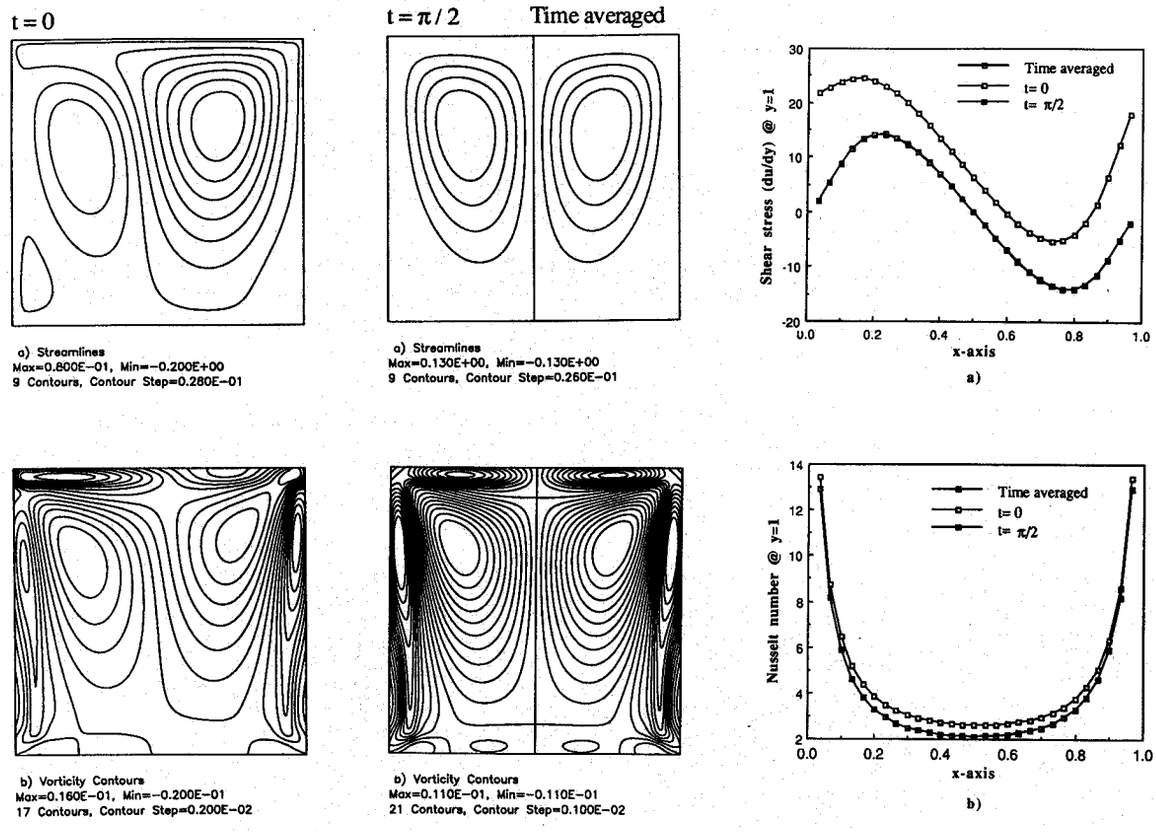

Fig. 5 Oscillatory cavity flow with heat transfer at $t = 0, \pi/2$, time-averaged, moving wall shear-stress distribution, and Nusselt number for $Ra = 10^3$, $Pr = Re = \beta = 1$.

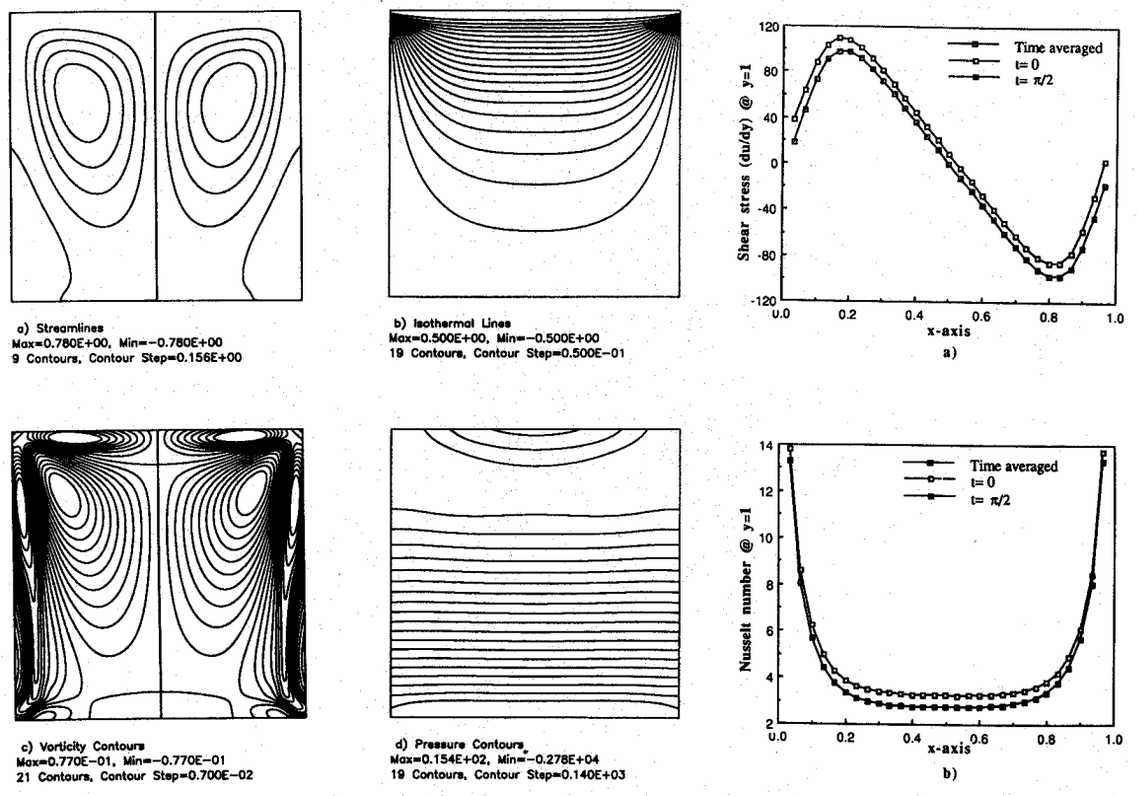

Fig. 6 Oscillatory cavity flow with heat transfer at $t = 0, \pi/2$, time-averaged, moving wall shear-stress distribution, and Nusselt number for $Ra = 10^4$, $Pr = Re = \beta = 1$.

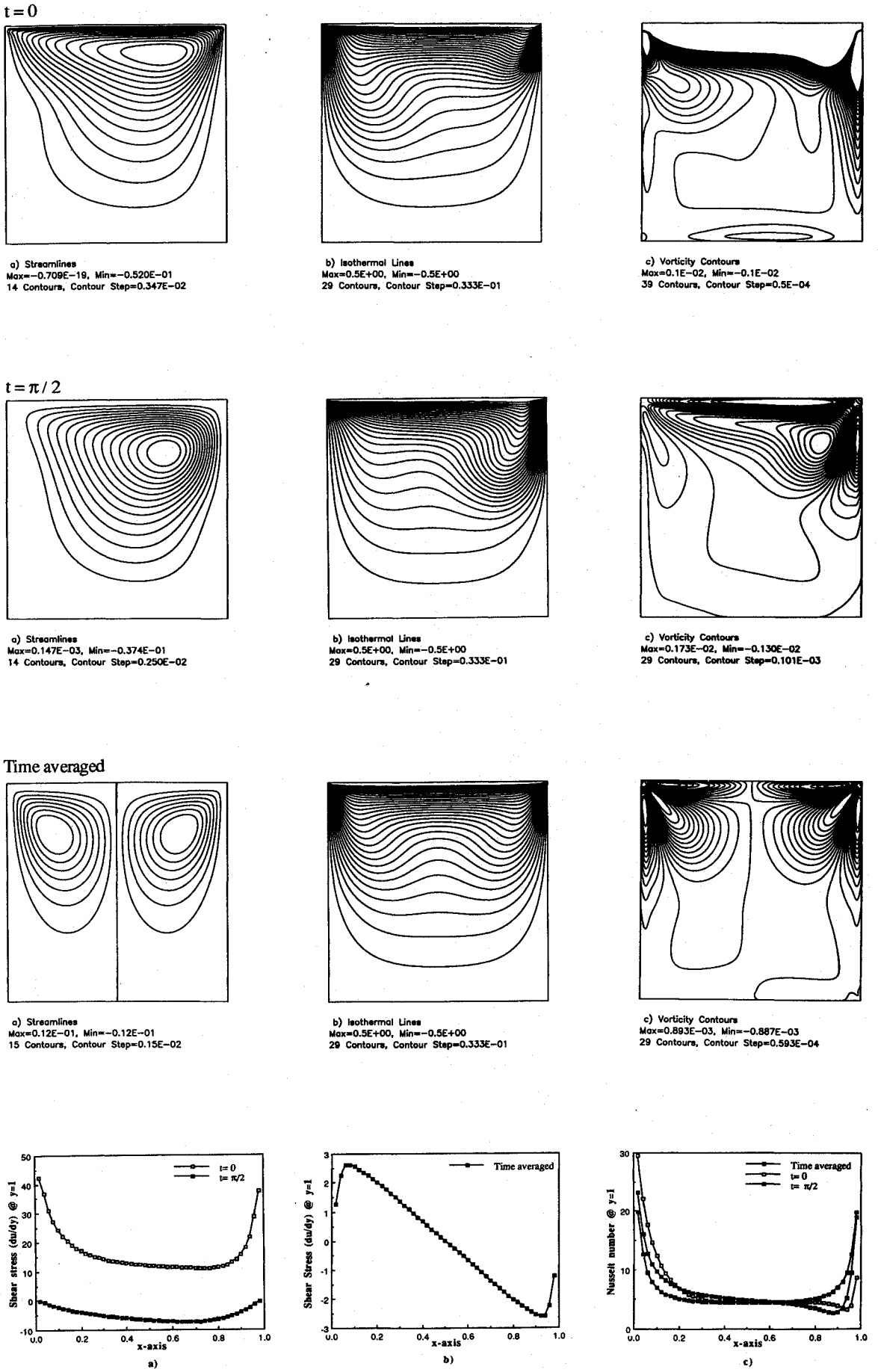

Fig. 7 Oscillatory cavity flow with heat transfer at $t = 0$, $\pi/2$, time-averaged, moving wall shear-stress distribution, and Nusselt number for $Ra = 10^4$, $Pr = 1$, and $Re = \beta = 200$.

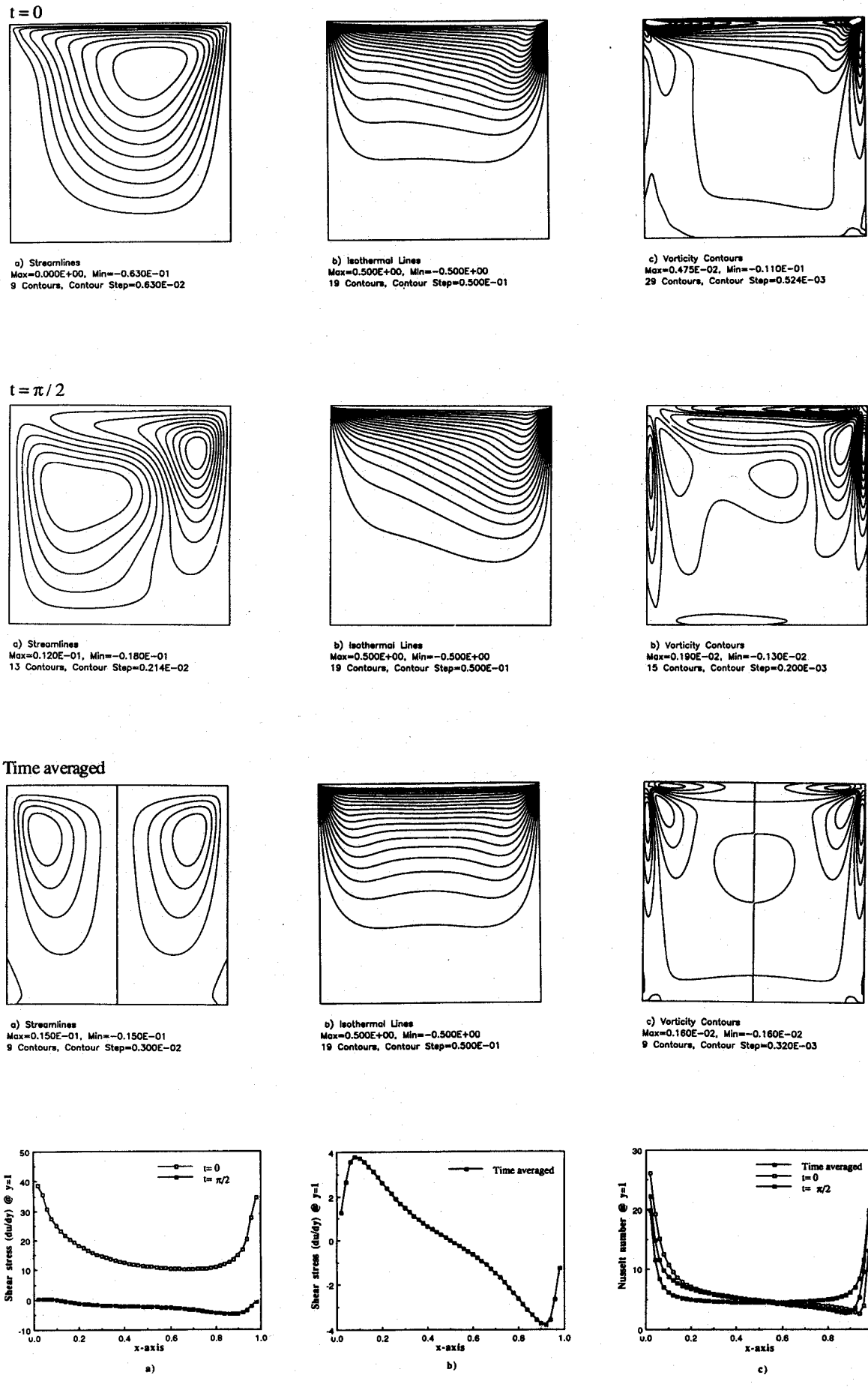

Fig. 8 Oscillatory cavity flow with heat transfer at $t = 0$, $\pi/2$, time-averaged, moving wall shear-stress distribution, and Nusselt number for $Ra = 10^5$, $Pr = 1$, and $Re = \beta = 200$.

into two major cases: one is $Pr = \beta = Re = 1$ for $Ra = 10^2$, 10^3, 10^4 and the other one is $Pr = 1$, $\beta = Re = 200$ for $Ra = 10^4$ and 10^5. A 30×30 uniform mesh of elements is used for former case and 50×50 uniform mesh of elements is used for the latter one. Problem definition is shown in Fig. 1(ii).

First we investigate the case $Pr = Re = \beta = 1$ for $Ra = 10^2$, 10^3, and 10^4. Computed results are shown in Figs. 4–6. From these results, it is clear that the main patterns of streamlines and vorticity contours are gradually affected by surface heating. At $Ra = 10^2$ the flow is mainly induced by lid-driven effect, so the flow pattern displays only the circulation created by the inertia effect. As Ra increases to 10^3, at $t = 0$ another vorticity appears and the original vorticity moves to the right and becomes smaller. When Ra is 10^4, the two vorticities become equal which means that thermal effect and lid-driven effect have equal influence. At $t = \pi/2$ the results are close to time averaged. This is due to $\beta = 1$ representing low frequency which means each step is approximately steady, so at $t = \pi/2$ and time averaged the zero moving wall velocity will create the same flow pattern. On the other hand, the temperature boundary condition is symmetric to the midsection and the low Re corresponding to low inertial effect does not affect the temperature field, so it is not varied with time and all the isothermal lines are the same as shown in Fig. 6b. From these results, it can be found that the moving wall shear-stress distribution changes very much with the increase of Rayleigh number. The Nusselt number is defined as

$$Nu = -\frac{\partial \theta}{\partial y} + u\theta \tag{28}$$

According to the above reason, all three cases have the similar pattern. The Nusselt number has a minimum at the midsection of cavity and approaches infinity at the corners.

The results of $Pr = 1$, $Re = \beta = 200$, $Ra = 10^4$, 10^5 are shown in Figs. 7 and 8. At $Ra = 10^4$ the inertial effect overcomes the natural convection effect, so the flow pattern and temperature field vary with the lid-driven velocity direction and only the circulation created by moving lid shear force exists in the flowfield. Owing to inertial effect, the shear stress and Nusselt number are not symmetric at $t = 0$, $\pi/2$. As $Ra = 10^5$ the thermal effect becomes important and the result depends on time very much. At $t = 0$ the moving lid velocity approaching maximum value, all the fluid domain is dominated by inertial terms. At $t = \pi/2$ the moving lid velocity approaching minimum value, the vorticity created by natural convection becomes larger and these two vorticities have equal strength. In this case, the problem is dominated by natural convection and inertial effect simultaneously. Therefore, the whole domain is sensitive to both factors and changes with their influences in the flowfield.

VI. Conclusions

The calculation of natural convection within a two-dimensional enclosure is undertaken using a time-split finite element technique. The primitive equations of motion and energy are solved along with a pseudopressure formulation similar to the SIMPLE algorithm. Computer storage requirements and computation times are less than those required for conventional finite element methods, which usually must solve large, sparse matrices. The numerical examples discussed in this paper indicate that in addition to its simplicity, the proposed scheme is capable of producing reasonably accurate results. Finally, it may be said that if a time-step iterative solver is used, the dissymmetry does not cause any difficulties and we anticipate such solutions will be useful in many applications. Moreover, the extension to three-dimensional flows will be the aim of future work.

Acknowledgments

The authors are grateful to Prof. S. Biringen, University of Colorado, Boulder for helpful discussions and to the two anonymous referees for their insightful comments.

References

[1]Sani, R. L., Gresho, P. M., Lee, R. L., and Griffiths, D. F., "The Cause and Cure (?) of the Spurious Pressure Generated by Certain FEM Solutions of the Incompressible Navier-Stokes Equations: Part 1," *International Journal of Numerical Methods in Fluids*, Vol. 1, 1981, p. 17–43.

[2]Taylor, C., and Hood, P., "A Numerical Solution of the Navier-Stokes Equations Using FEM Technique," *Computers and Fluids*, Vol. 1, 1973, pp. 73–100.

[3]Brezzi, F., "On the Existence, Uniqueness and Approximation of Saddle-Point Problems Arising from Lagrangian Multiplier," *R.A.I.R.O.*, Vol. 8, 1974, pp. 129–151.

[4]Bercovier, M., and Engelman, M., "A Finite Element for the Numerical Solution of Viscous Incompressible Flows," *Journal of Computational Physics*, Vol. 30, 1979, pp. 181–201.

[5]Hughes, T. J. R., Lui, W. K., and Brooks, A., "Finite Element Analysis of Incompressible Viscous Flows by the Penalty Function Formulation," *Journal of Computational Physics*, Vol. 30, 1979, pp. 1–60.

[6]Reddy, J. N., "On Penalty Function Methods in the Finite Element Analysis of Flow Problems," *International Journal of Numerical Methods in Fluids*, Vol. 2, 1982, pp. 152–171.

[7]Reddy, J. N., "Penalty-Finite-Element Analysis of 3-D Navier-Stokes Equation," *Computer Methods in Applied Mechanics and Engineering*, Vol. 35, 1982, pp. 87–106.

[8]Malkus, D. S., and Hughes, T. J., "Mixed Finite Element Methods-Reduced and Selective Integration Technique: A Unification of Concept," *Computer Methods in Applied Mechanics and Engineering*, Vol. 15, 1978, pp. 63–81.

[9]Engelman, M. S., Sani, R. L., Gresho, P. M., and Bercovier, M., "Consistent vs. Reduced Integration Penalty Methods for Incompressible Media Using Several Old and New Elements," *International Journal of Numerical Methods in Fluids*, Vol. 2, 1982, pp. 25–42.

[10]Donea, J., Giuliani, S., Laval, H., and Quartapelle, L., "Finite Element Solution of the Unsteady Navier-Stokes Equations by a Fractional Step Method," *Computer Methods in Applied Mechanics and Engineering*, Vol. 30, 1982, pp. 53–73.

[11]Gresho, P. M., Chan, S., Upson, C., and Lee, R. L., "A Modified Finite Element Method for Solving the Time-Dependent, Incompressible Navier-Stokes Equation," *International Journal of Numerical Methods in Fluids*, Vol. 14, 1984, pp. 557–598.

[12]Kim, J., and Moin, P., "Application of a Fraction-Step Method to Incompressible Navier-Stokes Equations," *Journal of Computational Physics*, Vol. 59, 1985, pp. 508–323.

[13]Ramaswamy, B., "Finite Element Solution for Advection and Natural Convection Flows," *Computers and Fluids*, Vol. 16, 1988, pp. 349–388.

[14]Ramaswamy, B., "Efficient Finite Element Method for Two-Dimensional Fluid Flow and Heat Transfer Problems," *Numerical Heat Transfer*, Vol. 17, 1990, pp. 123–154.

[15]Ramaswamy, B., Jue, T. C., and Akin, J. E., "Semi-Implicit and Explicit Finite Element Schemes for Coupled Fluid/Thermal Problems," *International Journal for Numerical Methods in Engineering*, in press.

[16]Ramaswamy, B., Jue, T. C., and Akin, J. E., "Finite Element Analysis of Unsteady Two-Dimensional Navier-Stokes Equations," *Numerical Heat Transfer*, in press.

[17]Temam, R., "On the Theory and Numerical Analysis of the Navier-Stokes Equations," North-Holland, Amsterdam, 1977.

[18]Beam, R. M., Warming, R. F., "An Implicit Factored Scheme for the Compressible Navier-Stokes Equations," *AIAA Journal*, Vol. 16, 1978, pp. 393–402.

[19]Gregoire, J. P., Benque, J. P., Lasbleiz, P., and Goussebaile, J., "3-D Industrial Flows Calculations by Finite Element Method," *Lecture Notes in Physics*, Vol. 218, 1985, pp. 245–249.

[20]MacCormack, R. W., "A Numerical Method for Solving the Equation of Compressible Navier-Stokes Equations," *AIAA Journal*, Vol. 20, 1982, pp. 1275–1281.

[21]Chorin, A. J., "Numerical Solution of the Navier-Stokes Equations," *Mathematics and Computations*, Vol. 22, 1968, pp. 745–762.

[22]Pelletier, D. H., Reddy, J. N., and Schetz, J. A., "Some Recent Developments and Trends in Finite Element Computational Natural Convection," *Annual Review of Numerical Fluid Mechanics and Heat Transfer*, Vol. 2, edited by C. L. Tien and T. C. Chawla, Hemisphere Publishing Corp., 1989, pp. 39–85.

[23]Reddy, J. N., "Penalty Function Methods in Conduction and Convective Heat Transfer," *Numerical Methods in Heat Transfer*, edited by E. Hinton, D. R. J. Owen, and C. Taylor, Pineridge Press, Swansea, 1983, pp. 155–202.

[24]De Vahl Davis, G., "Natural Convection on Air in a Square Cavity: A Benchmark Numerical Solution," *International Journal of Numerical Methods in Fluids*, Vol. 3, 1983, pp. 249–264.

[25]Biringen, S., and Danabasoglu, G., "Oscillatory Flow with Heat Transfer in a Square Cavity," *Physics of Fluids A*, Vol. 1, No. 11, 1989, pp. 1796–1812.

[26]Le Quere, P., and De Roquefort, T. A., "Computation of Natural Convection in Two-Dimensional Cavity with Chebyshev Polynomials," *Journal of Computational Physics*, Vol. 57, 1985, pp. 210–228.

[27]Markatos, N. C., and Pericleous, K. A., "Laminar and Turbulent Natural Convection in an Enclosed Cavity," *International Journal of Heat and Mass Transfer*, Vol. 27, 1984, pp. 755–772.